

1 Article

# 2 Performance evaluation and lubrication mechanism of 3 water-based nanolubricants containing nano-TiO<sub>2</sub> in 4 hot steel rolling

5 Hui Wu <sup>1</sup>, Jingwei Zhao <sup>1</sup>, Liang Luo <sup>2</sup>, Shuiquan Huang <sup>3</sup>, Lianzhou Wang <sup>4</sup>, Suoquan Zhang <sup>5</sup>,  
6 Sihai Jiao <sup>5</sup>, Han Huang <sup>3\*</sup> and Zhengyi Jiang <sup>1\*</sup>

7 <sup>1</sup> School of Mechanical, Materials, Mechatronic and Biomedical Engineering, University of Wollongong,  
8 Wollongong, NSW 2522, Australia

9 <sup>2</sup> Automotive Research Institute, Hefei University of Technology, Hefei 230009, China

10 <sup>3</sup> School of Mechanical and Mining Engineering, The University of Queensland, Brisbane, QLD 4072, Australia

11 <sup>4</sup> School of Chemical Engineering, The University of Queensland, Brisbane, QLD 4072, Australia

12 <sup>5</sup> Baosteel Research Institute (R&D Centre), Baoshan Iron & Steel Co., Ltd., Shanghai 200431, China

13 \* Correspondence: hwu@uow.edu.au (H. Wu), jzhao@uow.edu.au (J. Zhao), han.huang@uq.edu.au (H.  
14 Huang), jiang@uow.edu.au (Z. Jiang)

15

16 **Abstract:** Hot rolling tests of a low-alloy steel were conducted at a rolling temperature of 850 °C  
17 under different lubrication conditions, including benchmarks (dry condition and water) and water-  
18 based nanolubricants containing different concentrations of nano-TiO<sub>2</sub> from 1.0 to 8.0 wt%. The  
19 effects of nanolubricants on rolling force, surface roughness, thickness of oxide scale and  
20 microstructure were systematically investigated through varying nano-TiO<sub>2</sub> concentrations. The  
21 results show that the application of nanolubricants can decrease the rolling force, surface roughness  
22 and oxide scale thickness of rolled steels, and refine ferrite grains. In particular, the nanolubricant  
23 containing an optimal concentration (4.0 wt%) of nano-TiO<sub>2</sub> demonstrates the best lubrication  
24 performance, owing to the synergistic effect of lubricating film, rolling, polishing and mending  
25 generated by nano-TiO<sub>2</sub>.

26 **Keywords:** nano-TiO<sub>2</sub>; water-based nanolubricant; hot rolling; grain refinement

27

## 28 1. Introduction

29 With a growing number of concerns about energy crisis and environmental pollution in modern  
30 society, “Green Manufacturing” or “Environmentally Conscious Manufacturing” and its sustainable  
31 development are becoming increasingly more important in the field of engineering applications [1].  
32 Hot steel rolling, one of the most important manufacturing processes, has drawn considerable  
33 attention due to its huge energy consumption and pollutant emission. Previous studies have shown  
34 that the application of lubricants into hot steel rolling can lower the friction between work roll and  
35 workpiece [2-4], decrease rolling force [5, 6], reduce thickness of oxide scale [6-8], increase roll service  
36 life [9, 10], improve surface quality of rolled products [7, 8, 10], and refine grains in obtained  
37 microstructure [7, 8]. These thus reduce energy consumption, increase yield and production  
38 efficiency, improve the mechanical properties of rolled steels, and bring about great economic  
39 benefits.

40 Nowadays, conventional neat oil and oil-in-water (O/W) emulsions have still been used most  
41 commonly in the research of hot steel rolling [2-4, 6, 10-14]. For examples, Matsubara et al. [4]  
42 investigated the relationship between the film thickness and the coefficient of friction (COF) value in  
43 hot steel rolling by using neat lubricating oil instead of O/W emulsion on the work rolls in order to  
44 control the oil amount over a wide range. The results indicated that the COF decreased with the  
45 increase of oil film thickness up to around 0.2 μm, while it became constant even with a further

46 increase of oil film thickness at 700 °C. The former was ascribed to the presence of dry lubrication area  
47 coupled with boundary lubrication area. The latter, in contrast, was affected by a combination of  
48 boundary and hydrodynamic lubrication, which separated the work roll and the workpiece from  
49 direct contact. Azushima et al. [2, 3] developed a simulation testing machine for hot steel rolling to  
50 measure the COF and studied the lubrication mechanism using O/W emulsion with oil  
51 concentrations of 0-3.0 vol%. The results showed that the COF value decreased with the increase of  
52 oil concentration up to 1.0 vol%, while it remained constant when the oil concentration varied from  
53 1.0 to 3.0 vol%, owing to mixed lubrication regime and hydrodynamic lubrication, respectively. In  
54 another case, it has been reported that 1:1000 O/W emulsion appeared to maximally decrease rolling  
55 force and torque in hot steel rolling at a rolling temperature of 850 °C, compared to other rolling  
56 conditions such as dry, hot forging oil and 1:500 O/W emulsion [6]. Lenard et al. [12] also applied  
57 1:1000 O/W emulsion to study the COF variation by means of inverse calculations at rolling  
58 temperatures of 850, 900, 950 and 1000 °C. They found that the COF increased when the rolling  
59 temperature decreased or when the pressures on the strip increased, and the COF tended to decrease  
60 when the rolling speed increased.

61 The application of lubricants that contain oil, however, inevitably causes environmental issues  
62 due to the inherent toxicity and nonbiodegradable nature of oil, especially when burnt and  
63 discharged during hot steel rolling process [15]. In this regard, a type of environment-friendly  
64 lubricant with excellent lubricating performance is urgently needed to substitute conventional oil-  
65 containing lubricants. In recent years, the research trend on water-based lubricants added with  
66 nanoparticles (NPs) is continuously ascending due to their excellent tribological properties and  
67 promising potential in hot steel rolling, even though the relevant reports are still scarce [8, 16-23]. For  
68 instance, Bao et al. [8] carried out hot steel rolling tests at temperatures of 750-950 °C using water-  
69 based lubricants containing SiO<sub>2</sub> NPs, and found that the use of as-prepared lubricants with the  
70 addition of 0.5 wt% nano-SiO<sub>2</sub> resulted in improved surface morphology, reduced oxide scale  
71 thickness, and refined grain size, compared to that of the base lubricant. The lubrication mechanisms  
72 were proposed to be the functions of micro-rolling, polishing and self-repairing of SiO<sub>2</sub> NPs. Zhu et  
73 al. [19] performed experimental investigation on lubrication performance of water-based lubricants  
74 containing TiO<sub>2</sub> NPs during hot steel rolling at 950-750 °C. The results showed that the rolling force  
75 decreased significantly in each pass with the application of lubricant added with 2.0 wt% TiO<sub>2</sub>, and  
76 the decreased extent of rolling force kept growing as the rolling temperature dropped continuously.  
77 The possible lubrication mechanism was supposed to be the formation of lubrication film on strip  
78 surface. The comprehensive lubrication effect of water-based nanolubricant on hot steel rolling  
79 together with the detailed lubrication mechanism and corresponding grain refinement mechanism,  
80 however, has not been fully understood.

81 In our previous study [22], the lubricating performance of water-based nanolubricants  
82 containing nano-TiO<sub>2</sub> applied in hot steel rolling has been analysed in terms of rolling force, surface  
83 roughness and oxide scale thickness of rolled steel with proposed lubrication mechanism. In the  
84 present work, the comprehensive lubrication effect of water-based nanolubricant containing nano-  
85 TiO<sub>2</sub> on hot steel rolling was further systematically investigated including the effect on  
86 microstructure of rolled steel surface. Both the lubrication mechanism and the grain refinement  
87 mechanism were proposed based on an advanced experimental technique.

## 88 2. Materials and Experimental Procedure

### 89 2.1 Materials

90 A low-alloy steel with yield stress of 345 MPa was used in this study. Its chemical compositions  
91 are listed in Table 1. The steel samples were machined to dimensions of 300 × 100 × 8 mm<sup>3</sup> with  
92 tapered edges in order for an easy roll bite. Grinding and polishing were then performed on steel  
93 surfaces to generate a consistent surface roughness (R<sub>a</sub>) of approximately 0.5 μm, which ensured the  
94 identical surface conditions. Before each hot rolling test, the samples were cleaned with acetone to  
95 remove the surface residuals such as debris and oil.

96

**Table 1** Chemical compositions of the studied low-alloy steel (wt%).

C	Si	Mn	Mo	Ni	Cr	P	S	Nb+V+Ti
0.16	0.25	1.5	0.007	0.006	0.02	0.015	0.004	<0.02

97 The applied water-based nanolubricants containing nano-TiO<sub>2</sub> consisted of TiO<sub>2</sub> NPs,  
 98 polyethyleneimine (PEI), glycerol and balanced water. PEI is a cationic polymer, which behaves as a  
 99 surfactant in the water-based suspensions to improve the dispersibility of TiO<sub>2</sub> NPs in water. Glycerol  
 100 is a colourless, odourless and viscous liquid that is used to enhance the viscosity of suspensions. The  
 101 detailed preparation process of the nanolubricants can be found in our previous study, and the  
 102 lubricants exhibited excellent dispersibility and stability [21]. The chemical compositions of as-  
 103 prepared nanolubricants in this study are outlined in Table 2. The dry condition and water were  
 104 adopted as benchmarks in comparison to nanolubricants containing different concentrations of nano-  
 105 TiO<sub>2</sub> varying from 1.0 to 8.0 wt%.

106

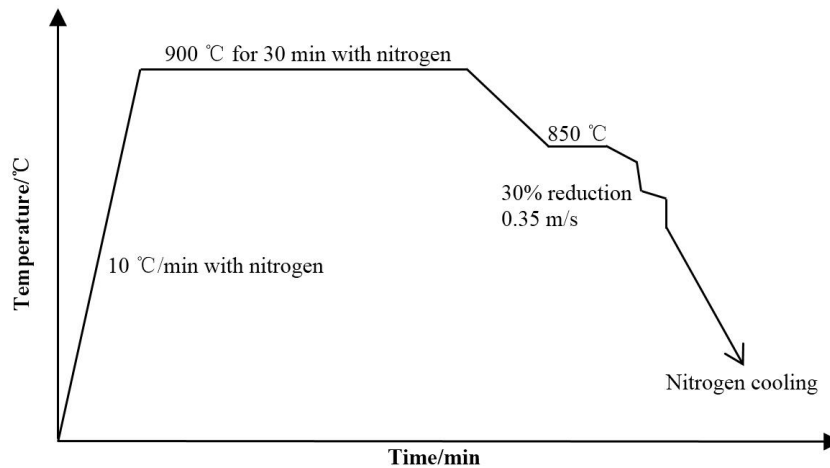
**Table 2** Chemical compositions of applied lubricants.

Lubrication type	Description
1	Dry condition
2	Water
3	1.0 wt% TiO <sub>2</sub> +0.01 wt% PEI + 10.0 vol% glycerol + balance water
4	2.0 wt% TiO <sub>2</sub> +0.02 wt% PEI + 10.0 vol% glycerol + balance water
5	4.0 wt% TiO <sub>2</sub> +0.04 wt% PEI + 10.0 vol% glycerol + balance water
6	8.0 wt% TiO <sub>2</sub> +0.08 wt% PEI + 10.0 vol% glycerol + balance water

107

## 2.2 Hot rolling tests

108 Hot rolling tests were carried out on a 2-high Hille 100 experimental rolling mill. The dimension  
 109 of work rolls is  $\Phi 225$  mm  $\times$  254 mm. Figure. 1 shows the hot rolling process of the low-alloy steel, in  
 110 which the steel samples were put into a high temperature electric resistance furnace and then heated  
 111 up to 900 °C for a holding period of 30 min with nitrogen flowing inside at a rate of 15 L/min. Later  
 112 on, the hot steel samples were rolled at 850 °C with a reduction of 30% and a rolling speed of 0.35 m/s  
 113 under different lubrication conditions mentioned in Table 2, followed by an immediate cooling  
 114 process in a sealed box full of nitrogen. The nitrogen used in hot rolling process aimed to refrain the  
 115 steel samples from being oxidised with air, which aided the analysis of lubrication effect on steel  
 116 oxidation. The lubricants were sprayed onto the pre-cleaned roll surface prior to each test until a  
 117 saturated layer of lubrication film was formed. The saturation can be defined hereby in terms of the  
 118 moment that the lubricants adhered onto roll surface began to drop down after formation of a  
 119 uniform and compact lubrication film. It should be noted that the capacity of absorption of various  
 120 lubricants on roll surface was inconsistent due to their different wettabilities. Two pieces of steel  
 121 samples were tested under the same rolling and lubrication conditions to obtain an average value for  
 122 a reasonable comparison of discrepant lubrication effectiveness.



123

124

Figure 1. The procedure of hot rolling testing.

### 125 2.3 Characterisation methodology

126 The rolling force during hot rolling was detected using two individual load cells assembled at  
 127 the drive and operation sides in the rolling mill. The data acquisition was conducted in a designed  
 128 program embedded in the MATLAB software.

129 The surface roughness of rolled steels was measured by a KEYENCE VK-X100K 3D Laser  
 130 Scanning Microscope. The measurement of surface roughness was primarily focused on the centre of  
 131 rolled steel surface by choosing five spots along the rolling direction to obtain average values.

132 The cross section of rolled steels along rolling direction was observed under a KEYENCE VK-  
 133 X100K 3D Laser Scanning Microscope. Epoxy resin was mounted onto the rolled steel surface before  
 134 cross-section observation in order to measure the oxide scale thickness. An FEI XT Nova NanoLab  
 135 200 which combines a dual beam of focused ion beam (FIB) and a high resolution field emission  
 136 scanning electron microscope (FESEM) was used to characterise the cross-section morphology of  
 137 rolled steel with further observation under a JEOL model JEM-ARM200F Transmission Electron  
 138 Microscope (TEM) coupled with an energy-dispersive spectrometer (EDS). The dual beam FIB is  
 139 equipped with a built-in platinum (Pt) gas injection system, which enables to form a thin layer of Pt  
 140 deposition onto the top of region of interest (ROI). The selection of ROI was directed following the  
 141 EDS mapping of Ti element obtained from FESEM.

142 The microstructure of rolled steels was observed under the 3D Laser Scanning Microscope, and  
 143 the ferrite grain size obtained was statistically analysed based on a microstructural model reported  
 144 by Luo et al [24]. The thermal conductivity of applied lubricants was measured in air at an ambient  
 145 temperature of 23.5 °C using a C-Therm TCi Thermal Conductivity Analyzer (C-Therm Technologies  
 146 Ltd., Canada). Each measurement was repeated ten times to obtain an averaged value.

## 147 3. Results

### 148 3.1 Lubrication effect on rolling force

149 Figure. 2 shows the rolling force obtained at a rolling temperature of 850 °C under different  
 150 lubrication conditions. It can be seen that the rolling force exhibits the highest value (605.2 KN) when  
 151 no lubrication is applied. In contrast, the use of water and water-based nanolubricants results in a  
 152 lower rolling force than that of dry condition. With the increase of concentration of nano-TiO<sub>2</sub>, the  
 153 rolling force decreases gradually until it arrives at the lowest value of 564 KN (caused by the  
 154 nanolubricant containing 4.0 wt% TiO<sub>2</sub>). Further increase of nano-TiO<sub>2</sub> concentration to 8.0 wt% leads  
 155 to slightly higher rolling force instead. In this case, 4.0 wt% TiO<sub>2</sub> acting as an optimal concentration  
 156 contributes to lowering the rolling force by 6.8%, compared to that of dry condition.

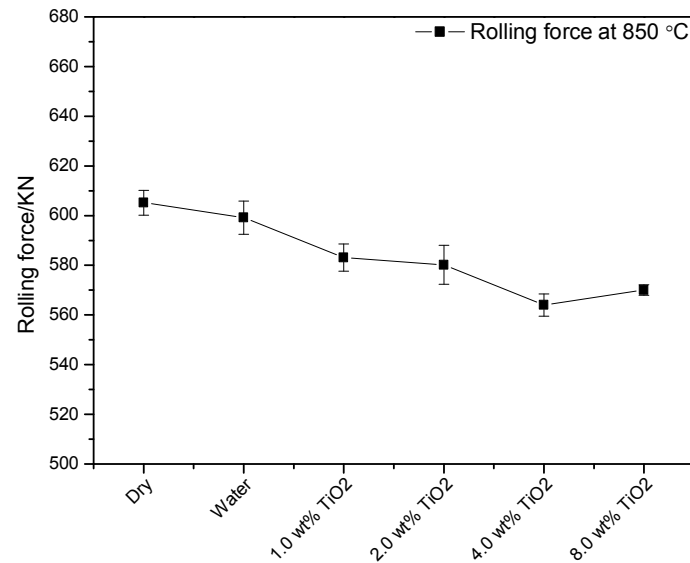


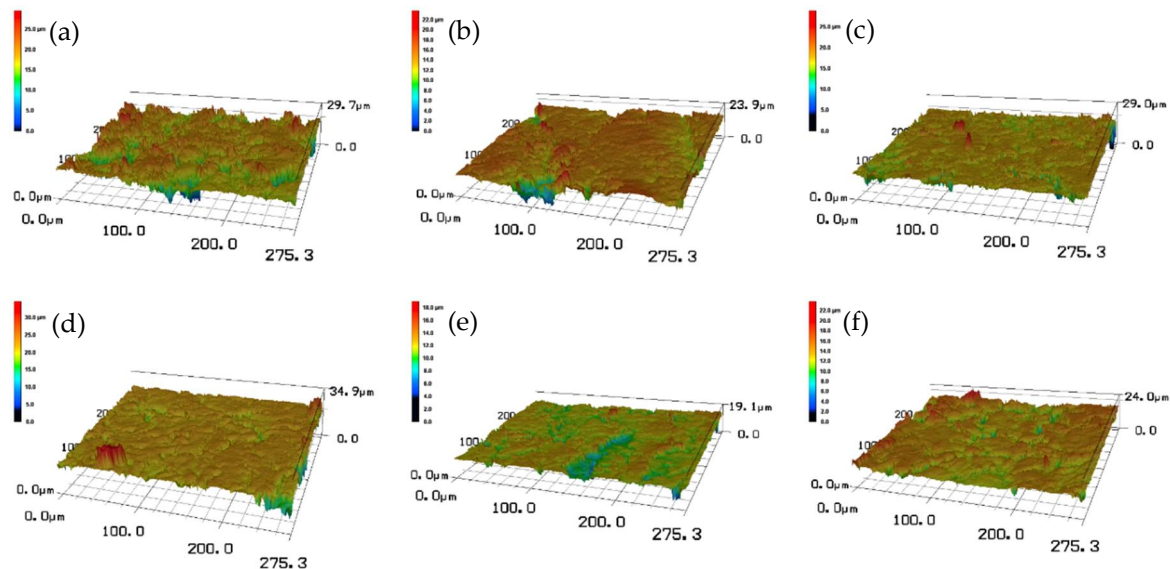
Figure. 2 Rolling force obtained at 850 °C under different lubrication conditions.

157

158

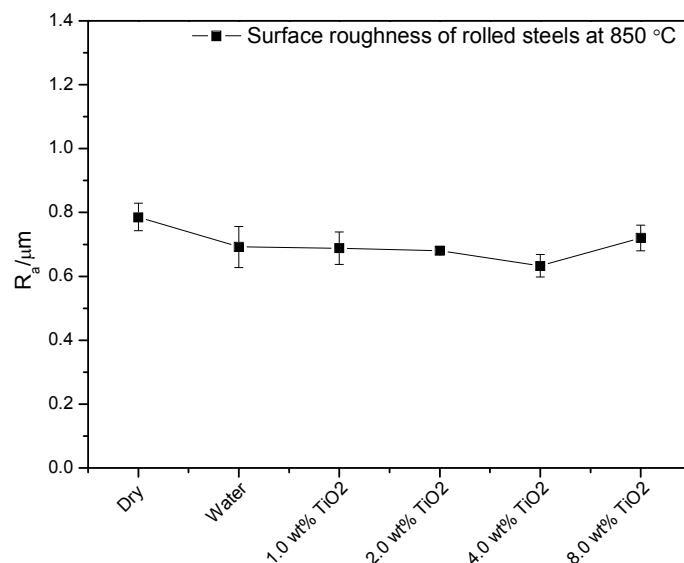
### 159 3.2 Lubrication effect on surface roughness

160 Figure. 3 shows the 3D profiles of surface morphologies of rolled steels at 850 °C under different  
 161 lubrication conditions. It is seen from Figure. 3(a) that the rolled surface with no lubrication displays  
 162 severe undulations with considerable peaks and valleys, indicating the roughest surface among all  
 163 of the rolled surfaces. Similarly, water lubrication brings forth comparable surface morphology to  
 164 that of dry condition with slightly better flatness, as shown in Figure. 3(b). Instead of these relatively  
 165 rough surfaces produced, however, the application of nanolubricant is inclined to flatten the surface  
 166 with increasingly higher concentration of nano-TiO<sub>2</sub> up to 4.0 wt% added into water before it yields  
 167 the smoothest rolled surface (Figure. 3(e)). However, a higher concentration of 8.0 wt% aggravates  
 168 the surface condition (Figure. 3(f)).



169 Figure. 3 3D profiles of surface morphologies of rolled steels at 850 °C under different lubrication conditions  
 170 of (a) dry, (b) water, (c) 1.0 wt% TiO<sub>2</sub>, (d) 2.0 wt% TiO<sub>2</sub>, (e) 4.0 wt% TiO<sub>2</sub> and (f) 8.0 wt% TiO<sub>2</sub>.

171 The effect of lubrication conditions on surface roughness of the rolled steels at 850 °C is shown  
 172 in Figure. 4. The varying trend of surface roughness corresponds to the surface morphologies  
 173 displayed in Figure. 3, suggesting that the optimal concentration of nano-TiO<sub>2</sub> in water-based  
 174 nanolubricants to improve the surface quality of rolled steel is 4.0 wt%.



175

176

Figure. 4 Surface roughness of rolled steels at 850 °C under different lubrication conditions.

177

### 3.3 Lubrication effect on oxide scale

178

179

180

181

182

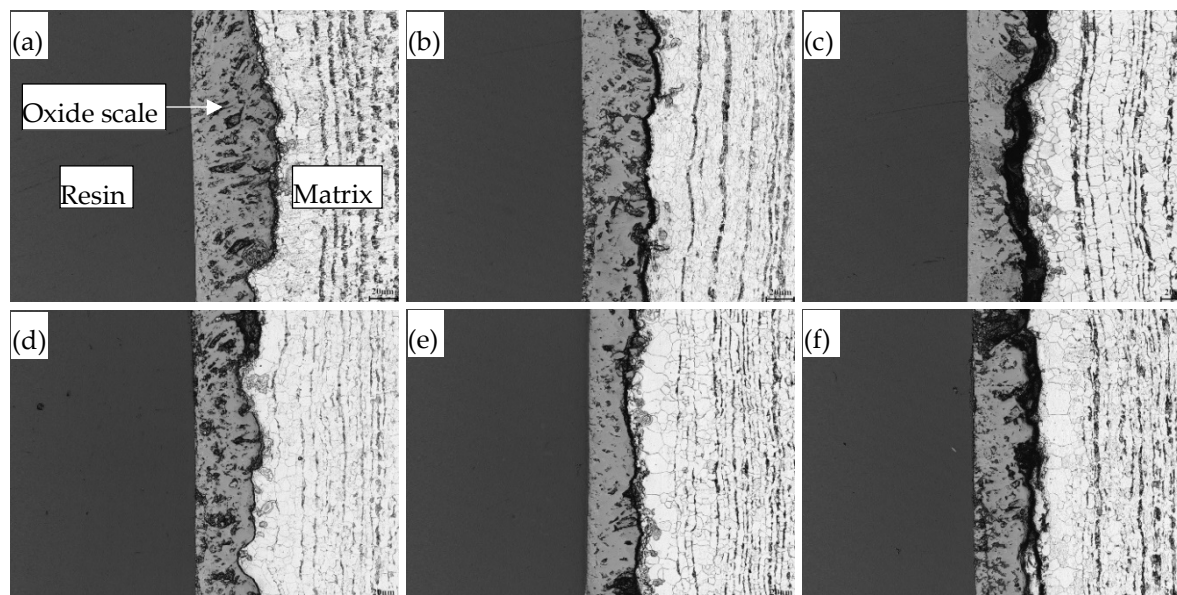
183

184

185

186

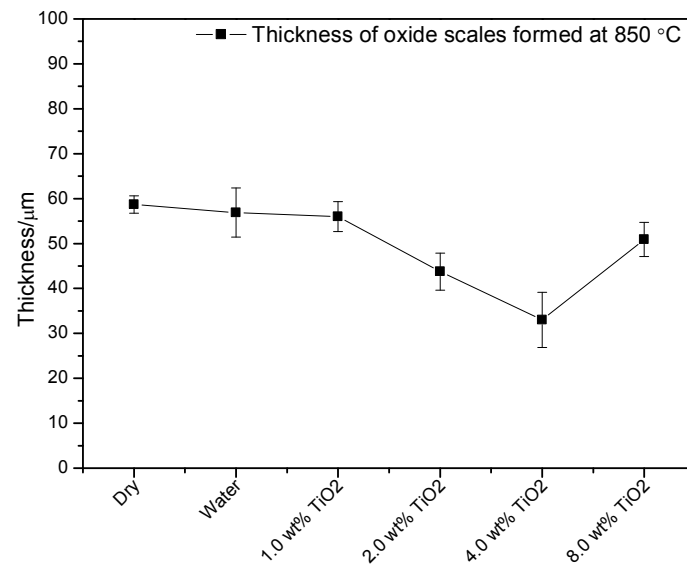
The morphologies of the oxide scales formed on the rolled steel at 850 °C under different lubrication conditions along cross sections are summarised in Figure. 5. It can be found that the thickness of oxide scales formed under dry condition and water is apparently reduced when water-based nanolubricants are applied, and the reduction of scale thickness is in proportion to the increase of nano-TiO<sub>2</sub> concentration from 1.0 to 4.0 wt%. When the nano-TiO<sub>2</sub> concentration continues to increase to 8.0 wt%, conversely, the scale thickness becomes thicker than that caused by nanolubricant containing 4.0 wt% TiO<sub>2</sub>. The statistic thickness values of oxide scale formed on rolled steel surface at 850 °C are shown in Figure. 6. Most importantly, the oxide scale thickness formed under dry condition can be maximally reduced by 43.8% under nanolubricant containing 4.0 wt% TiO<sub>2</sub>.



187

188

Figure. 5 Morphologies of oxide scales formed at 850 °C under lubrication conditions of (a) dry, (b) water, (c) 1.0 wt% TiO<sub>2</sub>, (d) 2.0 wt% TiO<sub>2</sub>, (e) 4.0 wt% TiO<sub>2</sub> and (f) 8.0 wt% TiO<sub>2</sub>.



189

190

Figure. 6 Thickness of oxide scales formed at 850 °C under different lubrication conditions.

191

### 3.4 Lubrication effect on surface microstructure and hardness

192

193

194

195

196

197

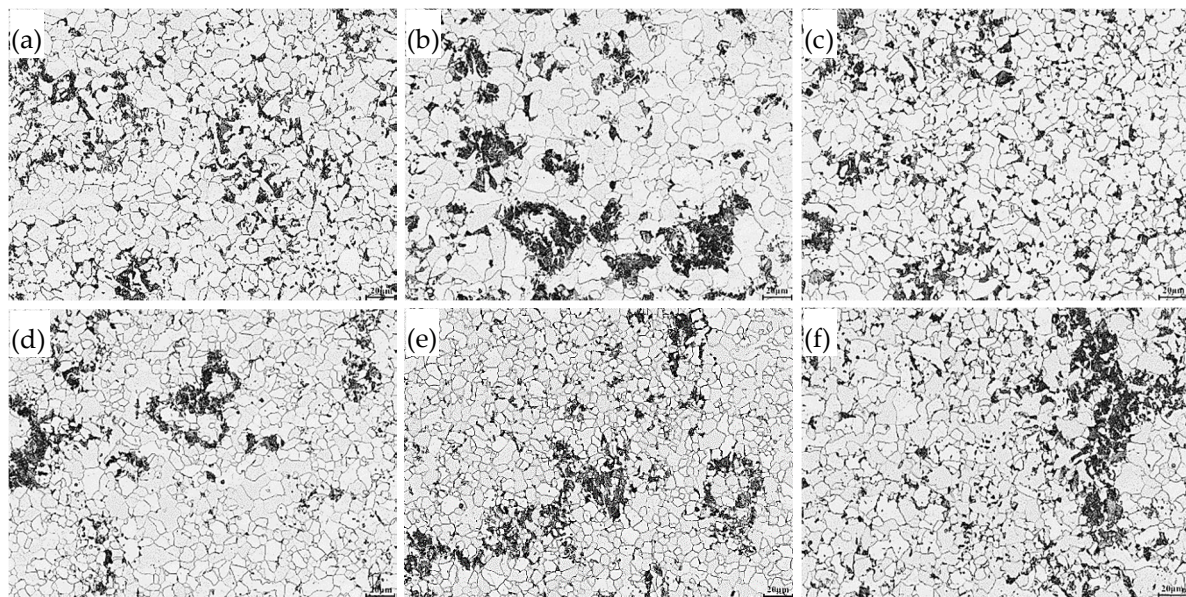
198

199

200

201

Figure. 7 demonstrates the surface microstructures of rolled steels at 850 °C under different lubrication conditions. It can be seen that the microstructure primarily consists of abundant polygonal ferrite (gray zones) and a small amount of pearlite (black zones). There is no significant change on the pearlite formed in terms of its amount and size. Nevertheless, it is of great interest that the ferrite grains obtained under dry condition and water lubrication can be refined to a large extent under nanolubrication, and especially nanolubricant containing 4.0 wt% TiO<sub>2</sub> leads to the finest ferrite grains, as shown in Figure. 7(e). The variation trend of grain refinement is consistent with those of rolling force (Figure. 2), surface roughness (Figure. 4) and thickness of oxide scale (Figure. 6). This clearly indicates that the water-based nanolubricant containing 4.0 wt% TiO<sub>2</sub> reveals the best lubrication effects on hot steel rolling at a rolling temperature of 850 °C.



202

203

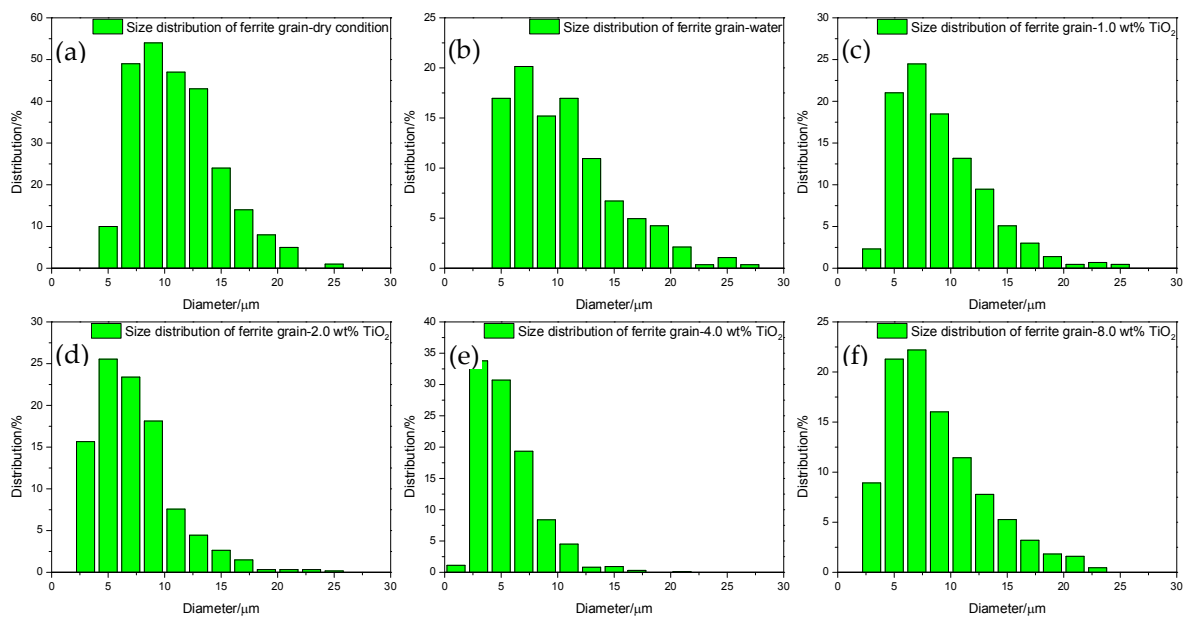
Figure. 7 Surface microstructures of rolled steels at 850 °C under different lubrication conditions of (a) dry, (b) water, (c) 1.0 wt% TiO<sub>2</sub>, (d) 2.0 wt% TiO<sub>2</sub>, (e) 4.0 wt% TiO<sub>2</sub> and (f) 8.0 wt% TiO<sub>2</sub>.

204

205

The size distributions of ferrite grains are statistically shown in Figure. 8, corresponding to the microstructures shown in Figure. 7. The statistical method of grain size can be referred to that

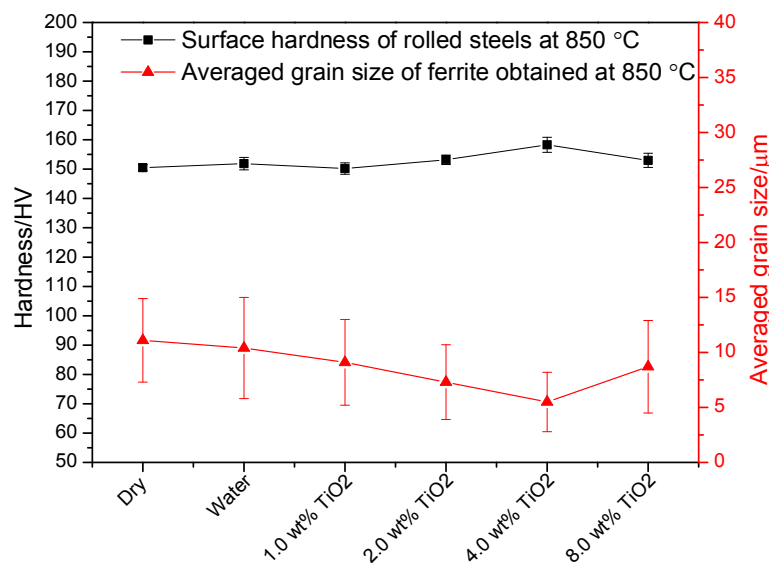
206 reported by Luo et al. [24], in which the grain shape is equivalent to be spherical. It can be clearly  
 207 seen that the majority of ferrite grains have diameters in the range of 7-13  $\mu\text{m}$  under lubrication  
 208 conditions of dry and water. In contrast, the grain size tends to become smaller and smaller with the  
 209 application of nanolubricants by increasing nano-TiO<sub>2</sub> concentration from 1.0 to 4.0 wt%. A further  
 210 increase of nano-TiO<sub>2</sub> concentration to 8.0 wt%, however, results in a slightly coarser grain size. The  
 211 averaged grain size of ferrite obtained at 850 °C under different lubrication conditions is shown in  
 212 Figure. 9. It is found that dry condition triggers the coarsest averaged grain size of around 11.1  $\mu\text{m}$ ,  
 213 which is refined to approximately 5.5  $\mu\text{m}$  in diameter by using nanolubricant containing 4.0 wt%  
 214 TiO<sub>2</sub>. The variation trend of averaged grain size is in line with that of surface hardness, showing that  
 215 the finer the grain size is, the higher surface hardness will be. To sum up, the grain size is refined by  
 216 50.5%, leading to an improved surface hardness by 4.9%.



217

218

219 **Figure. 8** Size distributions of ferrite grains obtained after rolling at 850 °C under different lubrication  
 220 conditions of (a) dry, (b) water, (c) 1.0 wt% TiO<sub>2</sub>, (d) 2.0 wt% TiO<sub>2</sub>, (e) 4.0 wt% TiO<sub>2</sub> and (f) 8.0 wt% TiO<sub>2</sub>.



221

222 **Figure. 9** Surface hardness of rolled steels and averaged grain size of ferrite obtained at 850 °C under different  
 223 lubrication conditions.

224

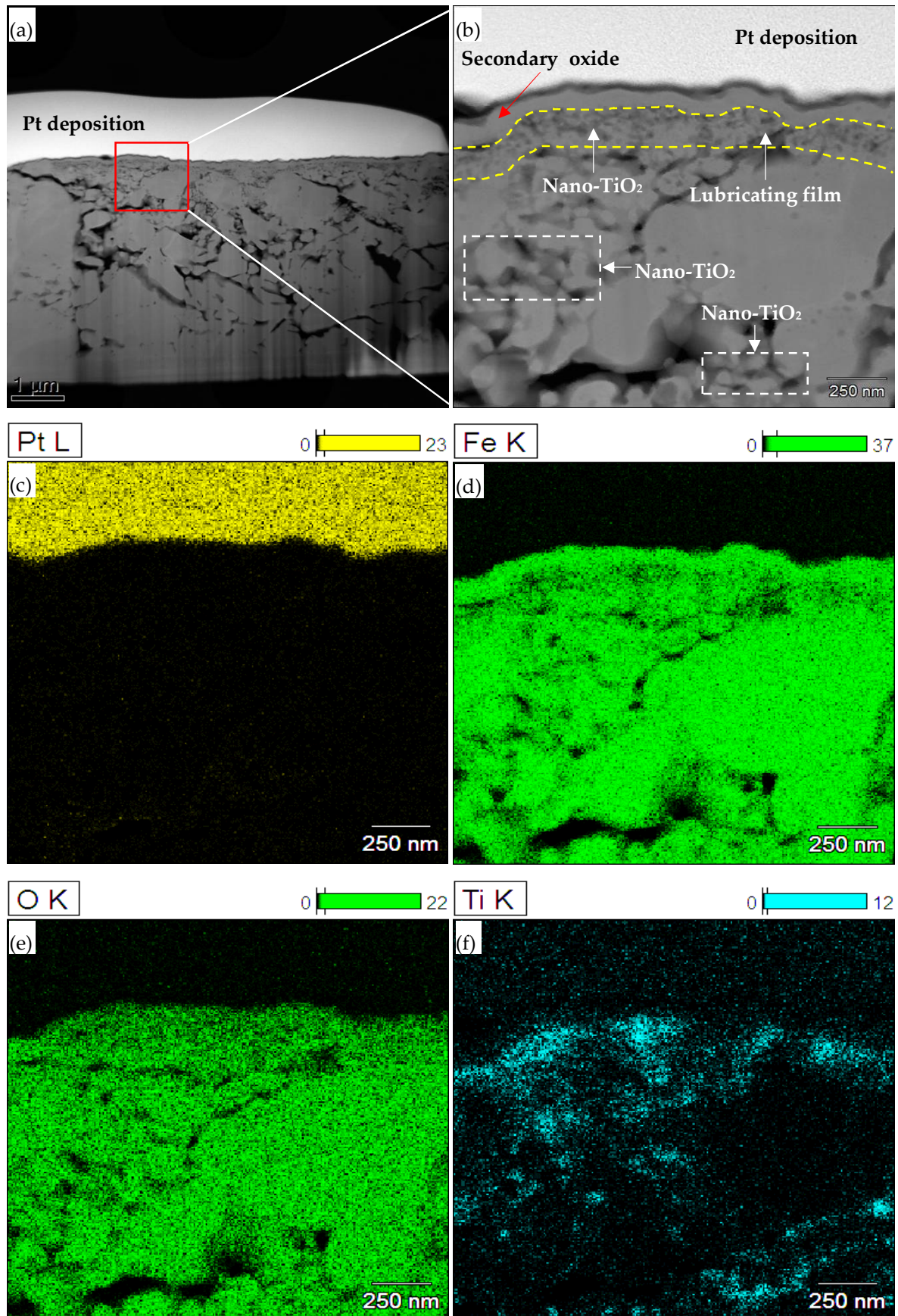
## 225 4. Discussion

### 226 4.1 FIB-TEM analysis

227 The TEM images of FIB foil cut from rolled steel surface and corresponding EDS mappings of  
228 typical elements obtained under 4.0 wt% TiO<sub>2</sub> lubrication at 850 °C are shown in Figure. 10. It can be  
229 seen from Figure. 10(a) that there is a clear interface between the Pt-deposition layer and the oxide  
230 scale layer, and the cross section of oxide scale has considerable defects including voids and cracks.  
231 The magnified area (red zone in Figure. 10(a)) at the interface is shown in Figure. 10(b). A secondary  
232 oxide scale layer with a thickness of approximately 0.06 μm exists at the top of oxide scale, which is  
233 formed due to the transfer of rolled steel from the runout table to the sealed nitrogen box.  
234 Furthermore, another layer (yellow zone) is generated underneath the secondary oxide scale layer,  
235 and the EDS mappings displayed in Figure. 10(e) and (f) indicate that the layer is full of TiO<sub>2</sub> NPs  
236 behaving as a “lubricating film”. Meanwhile, the spherical TiO<sub>2</sub> NPs in the lubricating film layer are  
237 able to act as bearing balls between the work roll and the workpiece, showing a “rolling effect”. Both  
238 the lubricating film and the rolling effect as thus contribute to decreasing the COF during the hot  
239 rolling process, which finally results in decrease of rolling force. In general, the lubrication effect on  
240 decreasing rolling force is dependent on effective amounts of well-dispersed TiO<sub>2</sub> NPs adhered onto  
241 the roll surface before rolling, which is determined by wettability and concentration of nanolubricant  
242 applied. In this case, the nanolubricant with better dispersibility, stronger wettability and higher  
243 concentration is more inclined to decrease rolling force to a larger extent. Many researchers have  
244 reported that the wettability of nanolubricant improves with increasing the concentration of NPs into  
245 base liquid [25-27]. Therefore, when the concentration of nano-TiO<sub>2</sub> is lower than 4.0 wt%, there are  
246 insufficient TiO<sub>2</sub> NPs left to form lubricating film and make rolling effect due to loss of nanolubricants  
247 when contacting the hot steel surface. When the concentration of nano-TiO<sub>2</sub> exceeds 4.0 wt% to a  
248 higher level of 8.0 wt%, instead, the rolling force varies at an opposite trend to present a higher value  
249 (see Figure. 2) because of the agglomeration of TiO<sub>2</sub> NPs [20, 21], which aggravates the friction  
250 between the work roll and the workpiece.

251 The white zone marked in Figure. 10(b) along with the EDS mappings shown in Figure. 10(e)  
252 and (f) indicates that TiO<sub>2</sub> NPs can also fill in the defects of steel surface during hot rolling process,  
253 exhibiting a “mending effect”. The mending effect hereby facilitates the decrease of surface roughness  
254 with similar principle to that of rolling force. While the difference is that the agglomeration of TiO<sub>2</sub>  
255 NPs induced by 8.0 wt% nano-TiO<sub>2</sub> lubrication may cause even deeper scratches than those produced  
256 by 4.0 wt% nano-TiO<sub>2</sub> lubrication, leading to higher surface roughness. This result has been proved  
257 in our previous study by using pin-on-disk tribological test [21]. The other reason of reducing surface  
258 roughness may be ascribed to the “polishing effect” of TiO<sub>2</sub> NPs, which helps to remove the bumps  
259 or peaks embedded in steel substrate and thus flatten the surface of rolled steel.

260 The formation of oxide scale during hot rolling process involves temperature, oxygen and water,  
261 and the possible reasons to generate different thickness under different lubrication conditions have  
262 been investigated in our previous study [22].

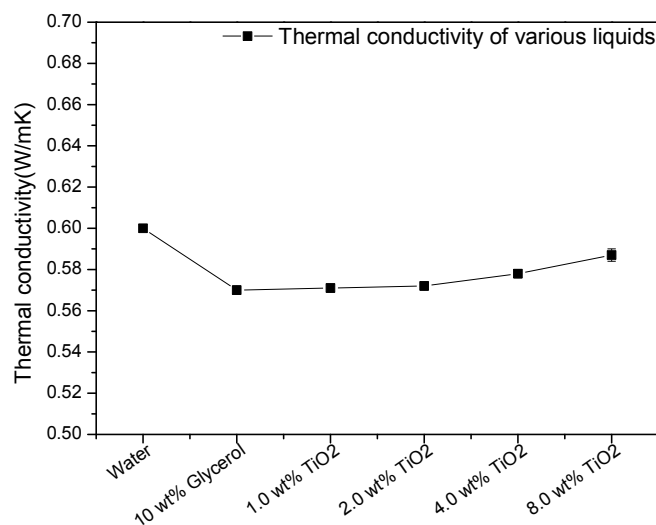


263 Figure 10 (a) TEM image of FIB foil cut from rolled steel surface, (b) TEM image of magnified area in (a), and  
 264 (c)-(f) EDS mappings of (b), under 4.0 wt% TiO<sub>2</sub> lubrication at 850 °C.

265  
 266

## 267 4.2 Grain refinement mechanism

268 It is well-known that controlling of nucleation and growth of grains is the fundamental method  
 269 for grain refinement. In general, the ferrite grain size decreases with the increase of cooling rate and  
 270 deformation of austenite in hot steel rolling [28]. Therefore, the critical influences on refining ferrite  
 271 grain in this study comprise cooling rate of applied lubricants and plastic deformation of steel strip.  
 272 The former is related to thermal conductivity of effective volume of lubricants adhered onto roll  
 273 surface, while the latter refers to the thickness reduction of steel strip. Figure. 11 shows the thermal  
 274 conductivity of nanolubricants measured in comparison to those of water and 10 wt% glycerol. It is  
 275 observed that water presents the highest thermal conductivity among all the liquids, showing a value  
 276 of around 0.6 W/mK at an ambient temperature of 23 °C [29]. A possible reason is that a concentration  
 277 of 10 wt% glycerol has very low thermal conductivity (0.29 W/mK) [30], which may greatly lower  
 278 down the thermal conductivity of water-based solutions. The thermal conductivity of nanolubricants,  
 279 however, increases with the increase of nano-TiO<sub>2</sub> concentration, which is consistent with the  
 280 findings reported by other researchers [31-34]. Although water displays a bit higher thermal  
 281 conductivity than water-based nanolubricants, it still leads to a lower cooling rate due to its poorer  
 282 wettability when adhering onto the roll surface before rolling. In this case, the cooling rate of  
 283 nanolubricants is higher than that of water, let alone that of dry condition, and it increases gradually  
 284 with the increase of nano-TiO<sub>2</sub> concentration based on the variation trend of wettability reported in  
 285 our previous study [22]. Thus, the ferrite grains obtained during hot rolling are supposed to be more  
 286 readily refined with the application of nanolubricants, compared to those of dry condition and water.  
 287 Besides, the nanolubricant containing higher nano-TiO<sub>2</sub> concentration is more likely to refine ferrite  
 288 grains.



289

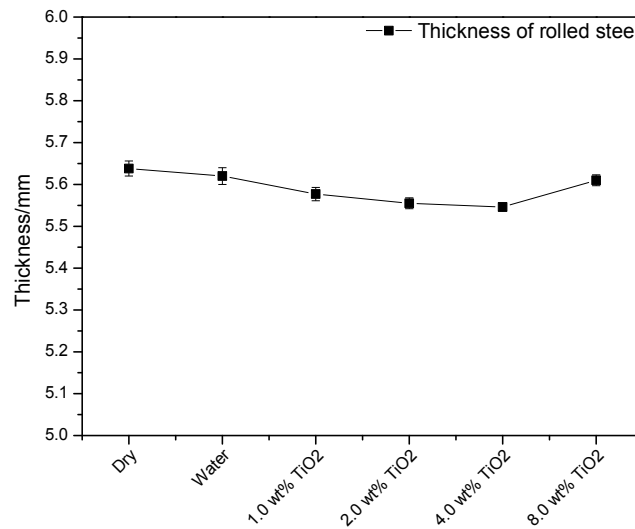
290 **Figure. 11 Thermal conductivity measured at ambient temperature as a function of various liquids.**

291 When it comes to the effect of plastic deformation on grain refinement, the exit thickness of rolled  
 292 steel needs to be considered. The relationship between exit thickness of rolled steel and rolling force  
 293 is normally referred to the Gaugemeter equation [35]:

$$294 \quad h = C_0 + P/K_s \quad (1)$$

295 where  $h$  is the exit thickness of rolled steel,  $C_0$  is the no-load roll gap,  $P$  is the rolling force, and  $K_s$  is  
 296 the mill structural stiffness. For the rolling test conducted on the same rolling mill under the same  
 297 rolling parameters,  $C_0$  and  $K_s$  are constant. In this case, a lower rolling force is inclined to induce a  
 298 thinner exit thickness of steel. The thickness values of rolled steel are shown in Figure. 12, the trend  
 299 of which is well matched with that obtained in Figure. 4. It can be seen that the use of nanolubricant  
 300 containing 4.0 wt% TiO<sub>2</sub> results in a rolled steel with the thinnest thickness (5.55 mm), compared to  
 301 those of other lubrication conditions, presenting the greatest deformation. As a whole, the combined

302 effects of cooling rate together with plastic deformation induce the finest ferrite grains under  
 303 nanolubrication with 4.0 wt% TiO<sub>2</sub>, as shown in Figures. 7 and 8.



304

305

**Figure. 12 Final thickness of rolled steel at 850 °C under different lubrication conditions.**

306

#### 4.3 Lubrication mechanism

307

308

309

310

311

312

313

314

315

316

317

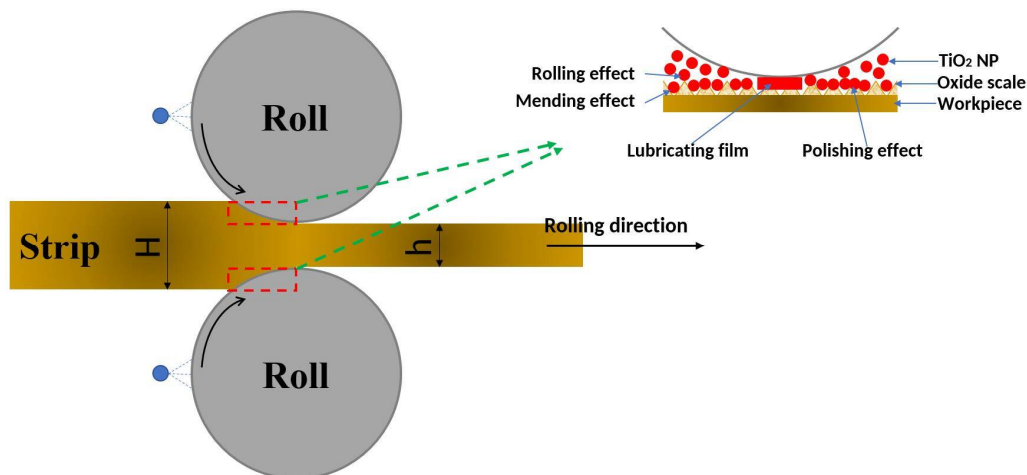
318

319

320

321

The lubrication mechanism using nanolubricants containing nano-TiO<sub>2</sub> in hot steel rolling is schematically illustrated in Figure. 13. When a work roll contacts a hot steel surface, the water-based nanolubricants adhered onto the roll surface are inclined to run off immediately at such a high rolling temperature of 850 °C. The retained nanolubricants simultaneously take lubrication effect in the contact area between the roll and the strip. On one hand, some of the TiO<sub>2</sub> NPs are able to spread over the strip surface to form lubricating film, and some others act as ball bearings, both of which contribute to the decreased COF during hot rolling, thereby decreasing the rolling force. The lubricating film can also isolate the air, leading to a decrease of oxide scale thickness. On the other hand, a number of TiO<sub>2</sub> NPs are committed to removing the bumps or peaks embedded in the strip substrate, showing a polishing effect. There are also considerable TiO<sub>2</sub> NPs that fill in the voids and cracks of strip surface, presenting a mending effect. The polishing effect combined with the mending effect thus contributes to reducing the surface roughness of rolled steels. The most interesting point is that the nanolubricants devote themselves to refining ferrite grains obtained during hot rolling, which is ascribed to the higher thermal conductivity of the nanolubricants and larger plastic deformation of strip steels, as discussed in Section 4.2.



322

323

324

**Figure. 13 Schematic illustration of lubrication mechanism using nanolubricants containing nano-TiO<sub>2</sub> in hot steel rolling at 850 °C.**

## 325 5. Conclusions

326 In this study, the hot steel rolling tests were performed at 850 °C under dry condition, water, and  
327 water-based nanolubricants containing nano-TiO<sub>2</sub> concentration varying from 1.0 to 8.0 wt%. The  
328 lubrication effects of the nanolubricants on rolling force, surface roughness, thickness of oxide scale  
329 and microstructure were systematically investigated. The below conclusions can be drawn.

- 330 (1) The rolling force obtained under dry condition is the highest among all the tests, which can be  
331 reduced maximally by 6.8% to 564 KN when nanolubricant containing 4.0 wt% nano-TiO<sub>2</sub> is  
332 applied.
- 333 (2) The surface roughness of the rolled steels under dry condition can be improved by 19.5% when  
334 using the nanolubricant with 4.0 wt% nano-TiO<sub>2</sub>. The lubricant also produces the flattest steel  
335 surface after hot rolling.
- 336 (3) The nanolubricant containing 4.0 wt% TiO<sub>2</sub> produces the thinnest oxide scale, which is 43.8%  
337 thinner than that obtained under dry condition.
- 338 (4) The use of nanolubricant containing 4.0 wt% TiO<sub>2</sub> leads to the grain refinement to the largest  
339 extent, showing 50% finer ferrite grain size than that of dry condition.
- 340 (5) The lubrication mechanism of water-based nanolubricant containing nano-TiO<sub>2</sub> in hot steel  
341 rolling is ascribed to the synergistic effect of lubricating film, rolling, polishing and mending.

342 **Author Contributions:** Hui performed the experiments in addition to analysing the data and writing the paper;  
343 Jingwei contributed the supervision and proofreading; Liang contributed the grain size statistics; Shuiquan  
344 contributed the preparation of lubricants; Lianzhou contributed dispersion stability of as-prepared lubricants;  
345 Suoquan contributed the supplies of steel samples; Sihai & Han contributed the project administration; Zhengyi  
346 contributed conceptualisation and supervision.

347 **Acknowledgments:** The authors acknowledge the financial support from Baosteel-Australia Joint Research and  
348 Development Centre (BAJC) under project of BA-17004 and Australian Research Council (ARC) under Linkage  
349 Project Program (LP150100591). The authors wish to thank Mr. Stuart Rodd, Mr. Nathan Hodges and other  
350 technicians in the workshop of SMART Infrastructure Facility at University of Wollongong (UOW) for their great  
351 supports on samples machining and operation of hot rolling mill. We also wish to thank Dr. Charlie Kong for  
352 his technical assistance and use of facilities supported by AMMRF at the Electron Microscope Unit at University  
353 of New South Wales. We also appreciate the kind assistance from Dr. David Mitchell at Electron Microscopy  
354 Centre at UOW on TEM observations. We finally would like to extend special thanks to Prof. Jun Chen at the  
355 Australian Institute for Innovative Materials at UOW for his great effort on measurement of thermal  
356 conductivity.

357 **Conflicts of Interest:** The authors declare no conflict of interest.

## 358 References

- 359 1. Wu, H., *A study of novel nano-additive water-based lubrication in hot rolling of steels*. PhD thesis, University of  
360 Wollongong, 2017.
- 361 2. Azushima, A., W.D. Xue, and Y. Yoshida, *Lubrication mechanism in hot rolling by newly developed simulation*  
362 *testing machine*. *Cirp Annals-Manufacturing Technology*, 2007. **56**(1): p. 297-300.
- 363 3. Azushima, A., W.D. Xue, and Y. Yoshida, *Influence of Lubricant Factors on Coefficient of Friction and*  
364 *Clarification of Lubrication Mechanism in Hot Rolling*. *Isij International*, 2009. **49**(6): p. 868-873.
- 365 4. Matsubara, Y., T. Hiruta, and Y. Kimura, *Effect of oil film thickness on lubrication property in hot rolling*. *ISIJ*  
366 *International*, 2015. **55**(3): p. 632-636.
- 367 5. Williams, K. *Tribology in Metal Working±New Developments, I*. in *Mech. E. Conf. Publications*, London, UK. 1980.
- 368 6. Shirizly, A. and J.G. Lenard, *The effect of lubrication on mill loads during hot rolling of low carbon steel strips*.  
369 *Journal of Materials Processing Technology*, 2000. **97**(1-3): p. 61-68.
- 370 7. Meng, Y., et al., *The Role of Nano-TiO<sub>2</sub> Lubricating Fluid on the Hot Rolled Surface and Metallographic Structure*  
371 *of SS41 Steel*. *Nanomaterials (Basel)*, 2018. **8**(2): p. 111.

- 372 8. Bao, Y., J. Sun, and L. Kong, *Effects of nano-SiO<sub>2</sub> as water-based lubricant additive on surface qualities of strips*  
373 *after hot rolling*. Tribology International, 2017. **114**: p. 257-263.
- 374 9. Spuzic, S., et al., *Wear of hot rolling mill rolls: an overview*. Wear, 1994. **176**(2): p. 261-271.
- 375 10. Beese, J.G., *Lubrication of hot-strip-mill rolls*. Wear, 1973. **23**(2): p. 203-208.
- 376 11. Barrett, C., *Influence of lubrication on through thickness texture of ferritically hot rolled interstitial free steel*.  
377 *Ironmaking & steelmaking*, 1999. **26**(5): p. 393-397.
- 378 12. Lenard, J.G. and L. Barbulovic-Nad, *The coefficient of friction during hot rolling of low carbon steel strips*. Journal  
379 *of tribology*, 2002. **124**(4): p. 840-845.
- 380 13. Matsuoka, S., et al., *Effect of lubrication condition on recrystallization texture of ultra-low C sheet steel hot-rolled*  
381 *in ferrite region*. ISIJ international, 1998. **38**(6): p. 633-639.
- 382 14. Yu, Y. and J.G. Lenard, *Estimating the resistance to deformation of the layer of scale during hot rolling of carbon*  
383 *steel strips*. Journal of Materials Processing Technology, 2002. **121**(1): p. 60-68.
- 384 15. Haus, F., J. German, and G.-A. Junter, *Primary biodegradability of mineral base oils in relation to their chemical*  
385 *and physical characteristics*. Chemosphere, 2001. **45**(6): p. 983-990.
- 386 16. He, A., et al., *The pH-dependent structural and tribological behaviour of aqueous graphene oxide suspensions*.  
387 *Tribology International*, 2017. **116**: p. 460-469.
- 388 17. He, A., et al., *Tribological Characteristics of Aqueous Graphene Oxide, Graphitic Carbon Nitride, and Their Mixed*  
389 *Suspensions*. Tribology Letters, 2018. **66**(1): p. 42.
- 390 18. He, A., et al., *Tribological Performance and Lubrication Mechanism of Alumina Nanoparticle Water-Based*  
391 *Suspensions in Ball-on-Three-Plate Testing*. Tribology Letters, 2017. **65**(2): p. 40.
- 392 19. Zhu, Z., et al., *Experimental research on tribological performance of water-based rolling liquid containing nano-*  
393 *TiO<sub>2</sub>*. Proceedings of the Institution of Mechanical Engineers, Part N: Journal of Nanoengineering and  
394 *Nanosystems*, 2014: p. 1740349914522455.
- 395 20. Wu, H., et al., *Friction and wear characteristics of TiO<sub>2</sub> nano-additive water-based lubricant on ferritic stainless*  
396 *steel*. Tribology International, 2018. **117**: p. 24-38.
- 397 21. Wu, H., et al., *A study of the tribological behaviour of TiO<sub>2</sub> nano-additive water-based lubricants*. Tribology  
398 *International*, 2017. **109**: p. 398-408.
- 399 22. Wu, H., et al., *Analysis of TiO<sub>2</sub> nano-additive water-based lubricants in hot rolling of microalloyed steel*. Journal  
400 *of Manufacturing Processes*, 2017. **27**: p. 26-36.
- 401 23. Yu, X., et al., *The role of oxide-scale microtexture on tribological behaviour in the nanoparticle lubrication of hot*  
402 *rolling*. Tribology International, 2016. **93**, **Part A**: p. 190-201.
- 403 24. Luo, L., Z. Jiang, and D. Wei, *Influences of micro-friction on surface finish in micro deep drawing of SUS304 cups*.  
404 *Wear*, 2017. **374-375**: p. 36-45.
- 405 25. Kasraei, S. and M. Azarsina, *Addition of silver nanoparticles reduces the wettability of methacrylate and silorane-*  
406 *based composites*. Braz Oral Res, 2012. **26**(6): p. 505-10.
- 407 26. Lim, S., et al., *Nanofluids Alter the Surface Wettability of Solids*. Langmuir, 2015. **31**(21): p. 5827-5835.
- 408 27. Vafaei, S., et al., *Effect of nanoparticles on sessile droplet contact angle*. Nanotechnology, 2006. **17**(10): p. 2523.
- 409 28. Tamura, I., H. Sekine, and T. Tanaka, *Thermomechanical processing of high-strength low-alloy steels*. 2013:  
410 Butterworth-Heinemann.
- 411 29. Ramires, M.L.V., et al., *Standard Reference Data for the Thermal-Conductivity of Water*. Journal of Physical and  
412 *Chemical Reference Data*, 1995. **24**(3): p. 1377-1381.
- 413 30. Tadjarodi, A. and F. Zabihi, *Thermal conductivity studies of novel nanofluids based on metallic silver decorated*  
414 *mesoporous silica nanoparticles*. Materials Research Bulletin, 2013. **48**(10): p. 4150-4156.

- 415 31. Cannio, M., et al., *Stabilization and thermal conductivity of aqueous magnetite nanofluid from continuous flows*  
416 *hydrothermal microwave synthesis*. *Materials Letters*, 2016. **173**: p. 195-198.
- 417 32. Kedzierski, M.A., et al., *Viscosity, density, and thermal conductivity of aluminum oxide and zinc oxide*  
418 *nanolubricants*. *International Journal of Refrigeration*, 2017. **74**: p. 3-11.
- 419 33. Özerinç, S., S. Kakaç, and A.G. Yazıcıoğlu, *Enhanced thermal conductivity of nanofluids: a state-of-the-art review*.  
420 *Microfluidics and Nanofluidics*, 2010. **8**(2): p. 145-170.
- 421 34. Zhu, H.T., et al., *Preparation and thermal conductivity of suspensions of graphite nanoparticles*. *Carbon*, 2007.  
422 **45**(1): p. 226-228.
- 423 35. Ginzburg, V.B., *Steel-rolling technology: theory and practice*. Marcel Dekker, Inc., 1989, 1989: p. 791.
- 424